International Journal of Research in Engineering and Innovation (IJREI)
Journal home page: https://ijrei.com/

RESEARCH PAPER

Effect of Zn/Mg Ratio on the Wear Behavior of Al–Zn–Mg Alloys

Ishu Verma[1], Dharmesh Kumar[1], Sk Md Iasin[2], Md. Basiruddin Sk[2], R. K. Jain[1], Jayanta Kumar Mahato[3]

[1]*School of Physical, Humanities and Mathematical Sciences, Shobhit Institute of Engineering & Technology (Deemed to-be University), Meerut, Uttar Pradesh, India.*
[2] *Department of Metallurgical and Material Engineering, Jadavpur University, Jadavpur, Kolkata, West Bengal, India.*
[3] *School of Electronics, Electrical & Mechanical Engineering, Shobhit Institute of Engineering & Technology (Deemed to-be University), Meerut, Uttar Pradesh, India.*

Article Information

Received: 17 August 2026
Revised: 23 October 2026
Accepted: 02 November 2026
Available online: 06 November 2026

Keywords:

Al–Zn–Mg alloys,
Zn/Mg ratio,
Stir casting,
Microstructure,
Coefficient of friction,
Wear rate,
Wear resistance

Abstract

The present study investigates the influence of Zn/Mg ratio on the microstructure and dry-sliding wear behaviour of stir-cast Al–Zn–Mg alloys. Five alloys with Zn/Mg ratios of 1.06, 1.93, 3.04, 4.07, and 5.08 were fabricated and evaluated through optical microscopy and pin-on-disc wear testing. The wear tests were conducted under a constant load, a sliding speed of 1 m/s and a sliding distance of 3015.92 m. Microstructural observations revealed dendritic morphology with secondary phases distributed along interdendritic regions and grain boundaries. The secondary-phase density increased up to a Zn/Mg ratio of 4.07 and subsequently decreased. Among the investigated alloys, AZM-4-1 (Zn/Mg ratio 4.07) exhibited the lowest and most stable coefficient of friction, the lowest wear rate and the highest wear resistance. In contrast, AZM-1-1 exhibited the highest wear rate and lowest wear resistance. The deterioration in wear performance at a Zn/Mg ratio of 5.08 indicates that increasing the ratio beyond an optimum level does not necessarily improve tribological properties.
2026 ijrei.com. All rights reserved

1. Introduction

Aluminium alloys are widely used in aerospace, automotive, transportation, and lightweight engineering applications owing to their low density, high specific strength, and ability to achieve enhanced mechanical properties through alloying and heat treatment. Among these materials, Al–Zn–Mg alloys are particularly attractive because of their excellent precipitation-hardening response. The combined addition of zinc (Zn) and magnesium (Mg) promotes the formation of nanoscale precipitates during artificial aging, which significantly improves hardness and resistance to plastic deformation. These characteristics make Al–Zn–Mg alloys promising candidates for components subjected to sliding contact and abrasive wear. However, their tribological performance depends strongly on alloy composition, heat-treatment conditions, precipitate distribution, and the resulting microstructure [1, 2]. The strengthening mechanism of Al–Zn–Mg alloys is primarily associated with the formation of $MgZn_2$-based precipitates during aging. Following solution treatment and rapid quenching, Zn and Mg remain in a supersaturated solid solution within the α-Al matrix. During subsequent aging, solute atoms and vacancies facilitate the formation of atomic clusters and Guinier–Preston (GP) zones, followed by metastable η′ precipitates and, under appropriate conditions, the equilibrium η phase, conventionally identified as $MgZn_2$. The precipitation sequence is commonly represented as supersaturated solid solution → GP zones → η′ → η-$MgZn_2$ [2-6]. Among these phases, the fine η′ precipitates are particularly important for achieving high hardness because their small dimensions, high number density, and interaction with dislocations effectively restrict plastic deformation.

Corresponding author: Jayanta Kumar Mahato
Email Address: jayant.mahato@shobhituniversity.ac.in
https://doi.org/10.36037/IJREI.2026.10607

Prolonged aging or exposure to higher temperatures may cause precipitate coarsening and transformation towards equilibrium phases, resulting in over-aging and a reduction in strengthening efficiency.

The Zn/Mg ratio is an important compositional parameter governing precipitation behavior because it influences solute availability, phase selection, precipitate evolution, and age-hardening kinetics. A change in this ratio can modify the relative populations of η′ and competing precipitate phases, even when the total Zn and Mg content remains constant. Zhang et al. [7-10] investigated Al–Zn–Mg–Zr alloys containing a fixed total Zn + Mg content of 6 wt% and Zn/Mg ratios of 1.6, 2.4, and 3.9. Their results demonstrated that increasing the Zn/Mg ratio changed the relative proportions of T′ and η′ precipitates. The measured η′ fraction increased from 25% to 61%, while the T′ fraction decreased from 75% to 39% across the investigated compositions. The maximum yield strength of 364 MPa was obtained at a Zn/Mg ratio of approximately 2.4, demonstrating that the optimum mechanical response depended on the balance between precipitate populations, their dimensions, and their distribution. These percentages represent the relative fractions of the identified precipitate populations and should not be interpreted as the volume fraction of $MgZn_2$ in the entire alloy. Nevertheless, this study establishes that the Zn/Mg ratio can significantly influence precipitation characteristics and mechanical performance [6, 7, 10].

The influence of Zn/Mg ratio on hardness is closely related to the size, number density, volume fraction, and interparticle spacing of the precipitates formed during aging. A high number density of fine η′ precipitates generally provide effective resistance to dislocation motion, resulting in increased hardness. However, the relationship between precipitate volume fraction and hardness is not necessarily linear because coarse precipitates and widely spaced particles may provide less effective strengthening than a finer and more uniformly distributed population. Furthermore, the equilibrium η phase and metastable η′ phase should not be considered equivalent in terms of their strengthening efficiency. Yang et al. [11] demonstrated that high-Zn/Mg Al–Zn–Mg alloys undergo composition-dependent precipitation evolution involving Zn-rich clusters, GP zones, and η′ precipitates. They also showed that the addition of Cu modified the precipitation pathway and affected the size and number density of η′ precipitates. These findings indicate that the influence of Zn/Mg ratio should be evaluated together with total alloying content and heat-treatment conditions rather than considered an independent predictor of hardness.

The relationship between precipitation hardening and wear resistance has been demonstrated experimentally by Rodinger et al. [1], who investigated the abrasive wear behavior of a precipitation-hardened Al–Zn–Mg alloy under different aging conditions. The alloy was solution-treated at 490 °C for 1 h and subsequently aged at different temperatures and durations. The maximum hardness of 227 HV1 was obtained after aging at 130 °C for 5 h, and this condition also exhibited the highest abrasive wear resistance among the investigated conditions. In contrast, aging at 190 °C for 9 h resulted in the lowest hardness and wear resistance. These results establish a direct relationship between the aging-dependent microstructure, hardness, and abrasive wear behavior. The improved wear resistance of the peak-aged alloy was associated with its greater resistance to surface deformation, while the reduced hardness of the over-aged condition contributed to increased susceptibility to material removal [1, 7, 8, 10-12].

From a tribological perspective, the improvement in hardness associated with fine precipitation is expected to reduce the extent of microploughing, microcutting, and plastic deformation during sliding or abrasive contact. When the matrix contains a dense and appropriately distributed population of strengthening precipitates, the surface becomes more resistant to the penetration and displacement of material by abrasive particles. Conversely, precipitate coarsening during over-aging may reduce the effectiveness of dislocation barriers and increase the susceptibility of the surface to deformation and wear. Nevertheless, wear resistance is not governed by hardness alone; applied load, sliding speed, counterface material, surface roughness, abrasive characteristics, and the formation of wear debris also influence the observed behavior. Therefore, the relationship between Zn/Mg ratio and tribological performance must be established by correlating composition and precipitation characteristics with experimentally measured wear rate and coefficient of friction.

Despite considerable research on precipitation strengthening in Al–Zn–Mg alloys, the quantitative relationship between Zn/Mg ratio, $MgZn_2$-based precipitate volume fraction, hardness, and wear resistance remains insufficiently established. In particular, the effects of Zn/Mg ratio on the volume fraction of metastable η′ and equilibrium η phases must be distinguished from changes in precipitate size, number density, and distribution. The existing literature provides evidence of composition-dependent precipitation and a strong relationship between aging-dependent hardness and abrasive wear, but these findings do not establish a universal Zn/Mg ratio that simultaneously maximizes hardness and minimizes wear rate. Accordingly, the present study aims to investigate the effect of Zn/Mg ratio on the tribological and wear behavior of Al–Zn–Mg alloys by examining the formation and distribution of $MgZn_2$-based precipitates and correlating their characteristics with hardness, coefficient of friction, and wear rate. The findings are expected to provide a microstructure-based understanding of the role of Zn/Mg ratio in optimizing the mechanical and tribological performance of Al–Zn–Mg alloys for lightweight engineering applications [1, 13-15].

2. Experimental Procedure

2.1. Fabrication of Al-Zn-Mg Alloys

Al-Zn-Mg alloys were fabricated by using HMI controlled stir casting machine (SwamEquip; SCM-Al01) as shown in Fig. 1(a). The alloys were fabricated by adding pure Zn and Mg major alloying elements in total ~80 gms (10 wt.%) with the pure Al of around 800 gm at 1:1, 2:1, 3:1, 4:1 and 5:1 Zn/Mg ratios. Initially, the necessary amount (~800 gm) of pure Al in small pieces were heated at 800±5°C into the melting furnace of stir casting machine and allow sufficient time to completely

melt the materials. After melting, the required amount (~80 gm) of Zn and Mg were added in-to the molten material and waited till completely melt of both Zn and Mg followed by continuous stirring through a mechanical stirrer blade. The stirrer blade was rotated at 650 rpm for 6-8 min and kept the auto-jog option on to get uniform mixing of alloying elements into the molten metal. After uniform mixing, the molten mixture metal was transferred into a preheated mould of cast iron having circular cross section cavity. Once solidified, the casted metal was removed from the mould cavity and cut in-to required shapes and sizes for further characterizations. The fabricated Al-Zn-Mg alloys are shown in Fig.1(b) and specimen codes of the corresponding Zn/Mg ratios are listed in Table 1. The actual Zn/Mg ratios corresponding to the nominal ratios of 1:1, 2:1, 3:1, 4:1, and 5:1 are 1.06, 1.93, 3.04, 4.07, and 5.08, respectively.

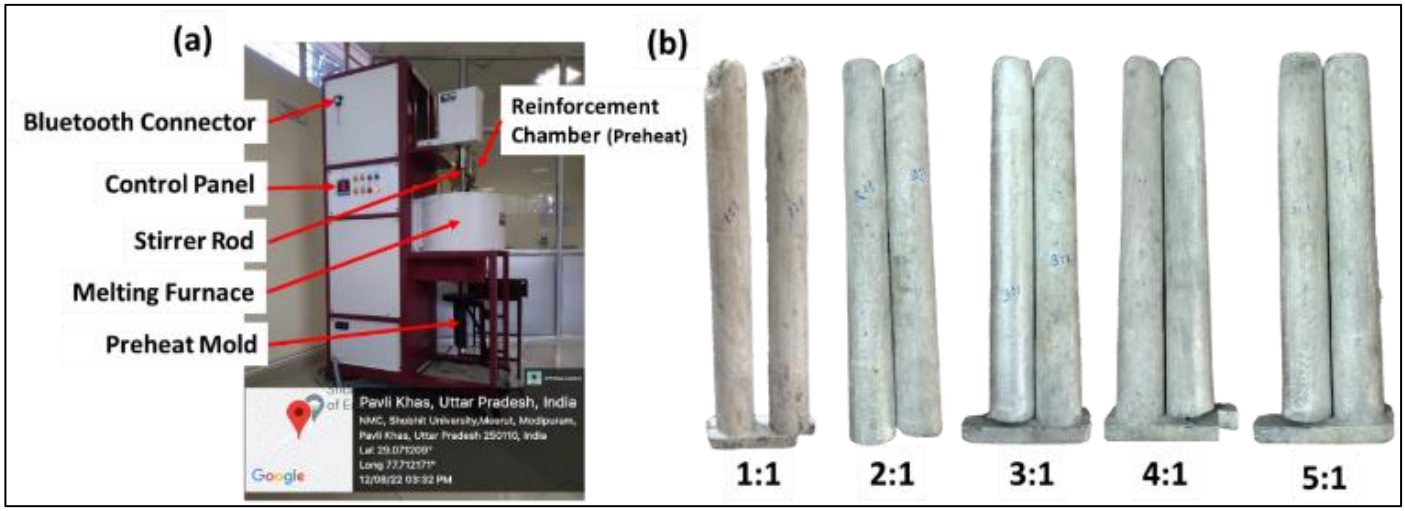


Figure 1: Photograph of (a) experimental set-up (Stir Casting Machine) for fabricating Al-Zn-Mg alloys and (b) fabricated Al-Zn-Mg alloys of five different Zn/Mg ratios.

Table 1. Specimen code with corresponding composition and grain size

Sl. No.	Specimen Code	Al (gm)	Zn (gm)	Mg (gm)	Zn/Mg Ratio	Average Grain Size (□m)
1	AZM-1-1	804.02	42.48	40.23	1.06	30
2	AZM-2-1	806.28	52.3	27.16	1.93	28
3	AZM-3-1	810.72	63.36	20.82	3.04	27
4	AZM-4-1	800.49	64.97	15.97	4.07	55
5	AZM-5-1	804.59	67.07	13.19	5.08	42

2.2. Microstructure Observations

The microstructures of fabricated alloys were investigated in an inverted metallurgical microscope (TRUEMET; RIM-5). The specimens were first cut into 10mm × 10 mm. Then, the small pieces were polished through a single-disk polisher by using successive grades of emery paper (600 grade to 2500 grade) followed by cloth polishing using micro-polish alumina (1-3 μm). The polished specimens were cleaned with ethanol followed by etching in Keller's agent for 30 seconds.

2.3. Wear Test

The dry sliding abrasive behavior of the fabricated Al-Zn-Mg alloys was assessed using a pin-on-disc type wear testing apparatus. Experiments were conducted in the holder-on-disc type Friction and Wear monitor (DUCOM; TR-20LE-M2) with data acquisition system at the Metallurgical & Materials Engineering Department, Jadavpur University, Kolkata, West Bengal. The load was applied on the sample by dead weight through pulley string arrangements. One kgf (9.80 N) load was applied on the specimens paced at track diameter of 30 mm on a rotating disc at 320 rpm and sliding speed of 1 m/s. The experimental parameters were kept constant for all AAMC specimens. The wear loss was calculated by weighing every specimen before and after the experiment using a high-accuracy digital balance. The weight difference was used to determine the wear rate using the equation:

$$\text{Wear Rate} = \frac{Mass\ Loss}{Sliding\ Distance} \quad (1)$$

$$\text{Specific Wear Rate} = \frac{Volume\ Loss}{Force * Sliding\ Distance} \quad (2)$$

$$\text{Wear Resistance} = \frac{1}{Wear\ Loss} \quad (3)$$

Where, Sliding Distance =3015.92 m, Force =9.81 N and density of Al alloys =2680 kg/m^3

3. Results and Discussions

3.1. Microstructure Observation

The microstructures of Al-Zn-Mg alloys having Zn/Mg ratios 1.06, 1.93, 3.04, 4.07 and 5.08 are shown in Fig. 2(a-e)

respectively. It is interestingly observed that the microstructure of AL-Zn-Mg alloys, irrespective of ratios between Zn and Mg shows the dendritic morphology consisting of secondary phases distributed in the inter-dendritic spacing as-well-as at the grain boundaries. These secondary phases are undissolved phases of Al, Zn and Mg which formed during the casting process [16]. Similar findings have been studied by Zhang et al. [16, 17]. They have stated that these phases have different crystallographic characteristics. Additionally, they have stated that at higher magnification these phases resemble a group of fish skeletons with stings and lumps of bone, which are known as secondary phases, as shown in Fig. 3(a-c) [16, 17]. It is clearly observed from Fig. 3(a-c) that the density of such secondary phases increases with an increase in Zn content up to a certain amount, i.e., from AZM-1-1 to AZM-4-1; however, such density again decreases at Al-Zn-Mg alloys with a higher content of Zn, i.e., in the case of AZM-5-1 alloy. Zhang et al. [17] have also reported similar observations. They have reported that Al-Zn-Mg alloys mainly consist of α-Mg phase and a small amount of $Mg_{32}(Al, Zn)_{49}$ phases, which are known as the T phase.

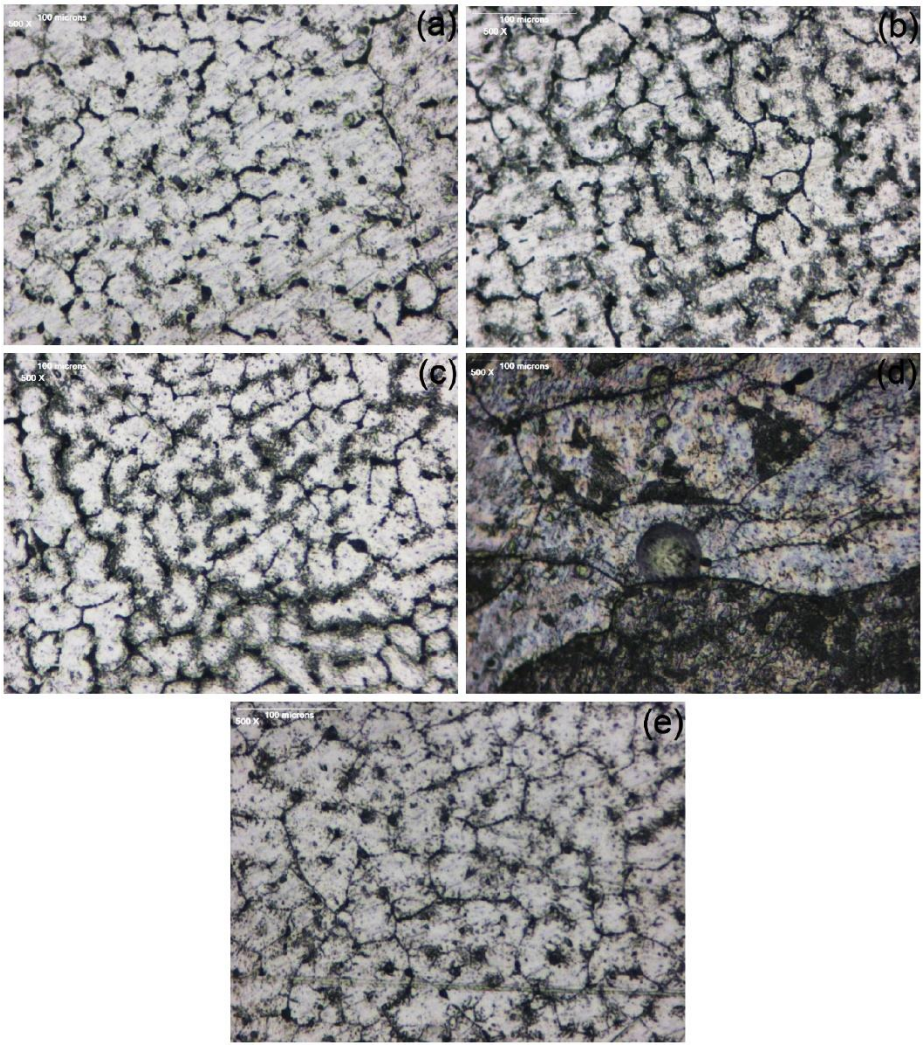


Figure. 2. Optical microstructure of AZM alloys having Zn/Mg ratio (a) 1.06, (b) 1.93, (c) 3.04, (d) 4.07 and (e) 5.08

They have also stated that with an increase in Zn content, the grain boundary becomes thicker, as the grain boundary areas of the alloy are dominated by wide, parallel-structured eutectic phases, which is consistent with the microstructure observation of the present investigation. Stemper et al. [18] have also investigated that $Mg_{32}(Al,Zn)_{49}$ phase (T phase) become metastable phase (T') at lower content of Zn and higher content of Mg in Al-Zn-Mg alloys. Zhao et al. [19] revealed that the coexistence of T' and η' phases (the metastable phase of $MgZn_2$) with a significant number density can result in the development of high-strength Al-Zn-Mg alloys. Following ASTM standard E112, the average grain sizes of Al-Zn-Mg alloys were measured from the optical microstructure as illustrated in Fig. 2(a-e), and are presented in Table 2. It has been found that, up to a certain amount, the average grain size of the alloys reduces as the Zn content increases and the Mg content concurrently decreases. This may be attributed to the formation of $MgZn_2$ phases and $Mg_{32}(Al, Zn)_{49}$, as these phases are associated with the wt.% concentration of both Zinc and Magnesium in Al-Zn-Mg alloys [17, 19].

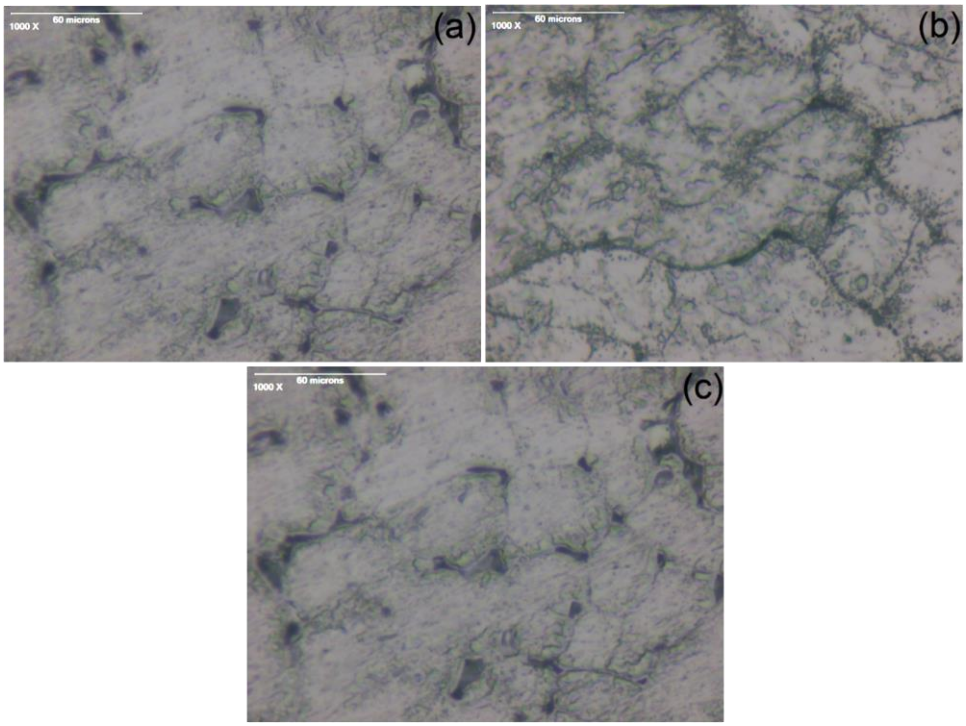


Figure 3. Optical microstructure of (a) AZM-1-1, (b) AZM-4-1 & (c) AZM-5-1 alloys at higher magnification.

3.2. Wear Behavior

Fig. 4 represents the variation in the coefficient of friction (COF) with cumulative sliding distance for the five fabricated alloys. The frictional response exhibits distinct differences in magnitude and stability, indicating the influence of material composition and surface interactions during sliding. AZM-2-1 exhibits the highest COF, fluctuating mainly around 0.95–1.10, with occasional peaks above 1.2. This behavior suggests greater frictional resistance, potentially associated with adhesive interactions, surface asperity interlocking, and the generation of wear debris at the sliding interface. In contrast, AZM-4-1 maintains the lowest and most stable COF, approximately 0.32–0.38, indicating the system has maximized its efficiency by reducing micro-level resistance and comparatively stable interfacial contact.

Fig. 4 illustrates the variation in coefficient of friction (COF) with cumulative sliding distance for the five specimens (AZM-1-1 to AZM-5-1). All specimens exhibit an initial running-in period, during which the COF fluctuates before approaching a relatively stable condition. AZM-2-1 exhibits the highest friction response, with COF fluctuating between approximately 0.95 and 1.15 and reaching a peak of nearly 1.30 during the initial sliding stage. AZM-3-1 shows an initial COF of approximately 0.80–0.95, followed by a gradual reduction from around 0.85 to 0.65 as the sliding distance increases to 3000 m. In comparison, AZM-4-1 maintains the lowest COF, remaining relatively stable between 0.32 and 0.38 throughout the test, indicating superior friction-reduction behaviour. AZM-5-1 exhibits intermediate friction characteristics, with COF values predominantly ranging from 0.55 to 0.70 after the initial running-in stage. The AZM-1-1 curve is not clearly distinguishable in the plotted data. Overall, the results indicate that AZM-4-1 provides the most favourable tribological performance, whereas AZM-2-1 experiences the highest frictional resistance. The relatively stable COF values at higher sliding distances suggest the establishment of a comparatively steady-state sliding condition.

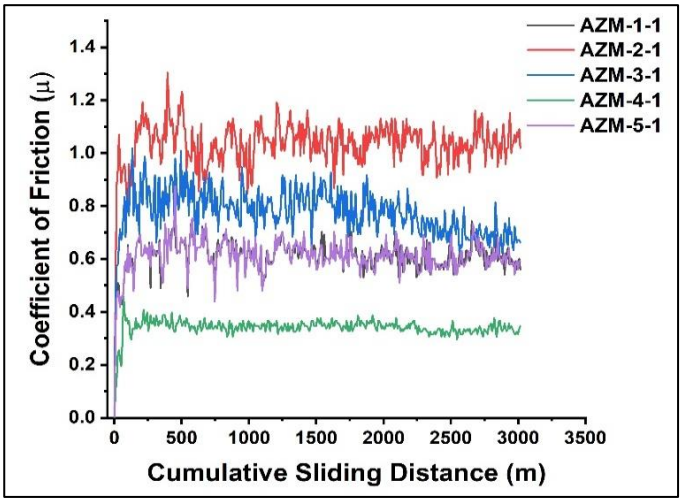


Figure 4. Variation of coefficient of friction with respect to sliding distance.

Fig. 5 illustrates the variation in wear rate and wear resistance for different specimens corresponding to different Zn/Mg ratios. AZM-1-1 exhibits the highest wear rate of approximately 9.9 kg/m, accompanied by a relatively low wear resistance of 3.3 kg^{-1}. For AZM-2-1, the wear rate decreases to approximately 6.6 kg/m, while wear resistance increases to 5.0 kg^{-1}. AZM-3-1 demonstrates a further reduction in wear rate to approximately 5.6 kg/m, with wear

resistance increasing to nearly 5.9 kg^{-1}. A significant improvement is observed for AZM-4-1, which exhibits the lowest wear rate of approximately 3.3 kg/m and the highest wear resistance of approximately 10.0 kg^{-1}, indicating superior wear performance. In contrast, AZM-5-1 shows an increase in wear rate to approximately 7.6 kg/m, accompanied by a reduction in wear resistance to approximately 4.3 kg^{-1}.

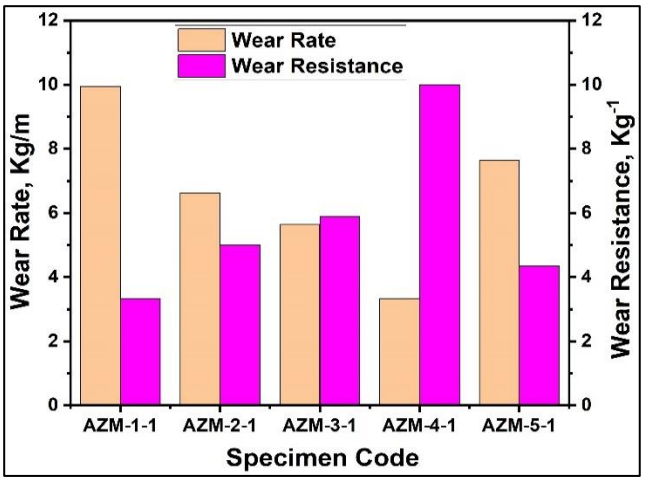


Figure 5. Variation of wear rate and wear resistance with respect to the Zn/Mg ratio.

Overall, AZM-4-1 demonstrates the most favourable tribological characteristics among the investigated specimens, whereas AZM-1-1 exhibits the poorest wear performance. These findings suggest that the Zn/Mg ratio plays an important role in determining the wear behaviour of the investigated alloys, with AZM-4-1 providing the optimum combination of low material loss and high wear resistance.

The comparatively low COF of AZM-4-1 suggests favorable sliding behavior, whereas the high COF of AZM-2-1 indicates greater frictional resistance. However, the persistent fluctuations in several curves suggest ongoing changes in interfacial contact. However, these mechanisms cannot be confirmed from the COF curves alone and require supporting worn-surface analysis, such as SEM and EDS.

The wear properties were calculated by following the concept of loss of mass as described in equations 1-3 and listed in Table 2. The variation of wear rate and wear resistance with respect to the variation of Zn/Mg ratio is represented in Fig. 5. It is interestingly observed that the wear rate decreases from approximately 9.9 kg/m for AZM-1-1 to 3.3 kg/m for AZM-4-1, while wear resistance increases to approximately 10 kg^{-1}. For AZM-5-1, the wear rate again rises to about 7.6 kg/m, accompanied by a reduction in wear resistance to approximately 4.3 kg^{-1}.

Table 2. Wear properties of Al-Zn-Mg alloys

Sl. No.	Specimen Code	Initial weight (gm)	Final weight (gm)	Sliding Distance (m)	Wear Rate (kg/m)	Specific Wear Rate (m^2/N)	Wear Resistance (kg^{-1})
1	AZM-1-1	3.829	3.826	3015.92	9.95e-10	3.78e-14	3.33e+05
2	AZM-2-1	4.016	4.014	3015.92	6.63e-10	2.52e-14	5e+05
3	AZM-3-1	4.4182	4.4165	3015.92	5.64e-10	2.14e-14	5.88e+05
4	AZM-4-1	3.718	3.717	3015.92	3.32e-10	1.26e-14	1e+06
5	AZM-5-1	3.4565	3.4542	3015.92	7.63e-10	2.9e-14	4.35e+05

These trends indicate that AZM-4-1 exhibits the most favourable wear performance among the investigated fabricated alloys. Such variation may be explained in terms of precipitation-controlled hardness and resistance to plastic deformation. A higher number density of fine, uniformly distributed η′ precipitates generally impede dislocation motion and improves resistance to material removal during sliding wear. However, precipitate coarsening, increased interparticle spacing or an unfavourable grain-boundary precipitate distribution may reduce strengthening efficiency. Yang et al. [11] demonstrated that Zn/Mg ratio influence precipitation evolution, including the formation of solute clusters, GP zones and η′ precipitates in Al–Zn–Mg alloys. These findings support the interpretation that the improved wear resistance observed up to AZM-4-1 may be associated with more effective precipitation strengthening, whereas the increased wear rate of AZM-5-1 may reflect less favourable microstructural conditions.

4. Conclusion

The present study investigates the effect of the Zn/Mg ratio on the microstructure and dry-sliding wear behavior of stir-cast Al–Zn–Mg alloys. Five alloy compositions with Zn/Mg ratios of 1.06, 1.93, 3.04, 4.07, and 5.08 were fabricated and systematically examined, yielding the following conclusion.

- All Al–Zn–Mg alloys exhibited dendritic microstructures with secondary phases distributed along interdendritic regions and grain boundaries.
- Secondary-phase density increased up to AZM-4-1 (Zn/Mg ratio 4.07) and decreased in AZM-5-1, while average grain size generally decreased with increasing Zn/Mg ratio up to an optimum level.
- AZM-4-1 exhibited the lowest and most stable coefficient of friction (0.32–0.38), indicating favorable sliding behavior.
- The wear rate decreased from approximately 9.9 to 3.3 kg/m, while wear resistance increased to approximately 10 kg^{-1} for AZM-4-1. Further increasing the Zn/Mg ratio to 5.08 deteriorated wear performance.
- The superior wear performance of AZM-4-1 may be associated with favorable grain structure, secondary-phase distribution, and precipitation strengthening.

References

[1] T. Rodinger, H. Lukšić, D. Ćorić, and V. Rede, "Abrasion wear resistance of precipitation-hardened Al-Zn-Mg alloy," *Materials,* vol.

17, no. 10, p. 2446, 2024.
[2] V. Hansen, O. Karlsen, Y. Langsrud, and J. Gjønnes, "Precipitates, zones and transitions during aging of Al-Zn-Mg-Zr 7000 series alloy," *Materials science and technology,* vol. 20, no. 2, pp. 185-193, 2004.
[3] L. Berg *et al.*, "GP-zones in Al–Zn–Mg alloys and their role in artificial aging," *Acta materialia,* vol. 49, no. 17, pp. 3443-3451, 2001.
[4] S. Liu *et al.*, "Revisiting the precipitation mechanisms of Guinier-Preston zones, η′, and η precipitates in Al-Zn-Mg alloys," *Acta Materialia,* vol. 268, p. 119789, 2024.
[5] G. Sha and A. Cerezo, "Early-stage precipitation in al–zn–mg–cu alloy (7050)," *Acta materialia,* vol. 52, no. 15, pp. 4503-4516, 2004.
[6] E. Thronsen *et al.*, "The evolution of precipitates in an Al–Zn–Mg alloy," *Journal of Materials Research and Technology,* vol. 23, pp. 5666-5680, 2023.
[7] X. Zhang *et al.*, "Quantitative analyses of Zn/Mg ratios on T'and η'precipitation strengthening and corrosion resistance in low alloyed Al-Zn-Mg-Zr alloys using atom probe tomography," *Materials Characterization,* p. 116486, 2026.
[8] H. Yin *et al.*, "Investigation on precipitate behavior and mechanical properties of Al-Zn-Mg-Cu alloys with various Zn/Mg ratios," *Journal of Materials Research and Technology,* vol. 33, pp. 5769-5783, 2024.
[9] Y. Zou *et al.*, "Investigation on microstructure and mechanical properties of Al-Zn-Mg-Cu alloys with various Zn/Mg ratios," *Journal of Materials Science & Technology,* vol. 85, pp. 106-117, 2021.
[10] Q. Zhu *et al.*, "Precipitation evolution of Al-Zn-Mg-Cu-(Ag) alloys with a low Zn/Mg ratio," *Journal of Materials Science & Technology,* vol. 195, pp. 177-196, 2024.
[11] M. Yang, S. Wang, M. Zhang, S. Liu, and L. Ye, "Aging hardening and precipitation behavior of high Zn/Mg ratio Al-Zn-Mg alloys with and without Cu," *Journal of Alloys and Compounds,* vol. 1022, p. 180017, 2025.
[12] Y. Li *et al.*, "Effect of Cu content and Zn/Mg ratio on microstructure and mechanical properties of Al–Zn–Mg–Cu alloys," *Journal of Materials Research and Technology,* vol. 19, pp. 3451-3460, 2022.
[13] J. Wang *et al.*, "Influence of Zn/Mg ratio on mechanical strength and corrosion resistance of Al-Zn-Mg alloys," *Journal of Alloys and Compounds,* vol. 1016, p. 178953, 2025.
[14] S. Chen, J. Li, G.-y. Hu, K. Chen, and L. Huang, "Effect of Zn/Mg ratios on SCC, electrochemical corrosion properties and microstructure of Al-Zn-Mg alloy," *Journal of Alloys and Compounds,* vol. 757, pp. 259-264, 2018.
[15] S.-J. Lin and K.-S. Liu, "Effect of aging on abrasion rate in an Al□ Zn□ Mg□ SiC composite," *Wear,* vol. 121, no. 1, pp. 1-14, 1988.
[16] H. Yin *et al.*, "Effect of Zn/Mg ratio on the microstructure and mechanical properties of as-cast Al–Zn–Mg–Cu alloys and the phase transformation during homogenization," *Journal of Materials Research and Technology,* vol. 26, pp. 3646-3660, 2023.
[17] J. Zhang, Z. Guo, F. Pan, Z. Li, X. J. M. S. Luo, and E. A, "Effect of composition on the microstructure and mechanical properties of Mg–Zn–Al alloys," vol. 456, no. 1-2, pp. 43-51, 2007.
[18] L. Stemper *et al.*, "Age-hardening of high pressure die casting AlMg alloys with Zn and combined Zn and Cu additions," vol. 181, p. 107927, 2019.
[19] P. Zhao *et al.*, "Effect of Zn/Mg ratio on microstructure and mechanical properties of Al-Zn-Mg alloys," vol. 312, p. 131676, 2022.

Cite this article as: Ishu Verma, Dharmesh Kumar, Sk Md Iasin, Md. Basiruddin Sk, R. K. Jain, Jayanta Kumar Mahato, Effect of Zn/Mg Ratio on the Wear Behavior of Al–Zn–Mg Alloys, International Journal of Research in Engineering and Innovation, 10 (6), (2026), 327-333. https://doi.org/10.36037/IJREI.2026.10607.